# Applying Digital Hydraulic Technology on a Knuckle Boom Crane

Viktor Donkov[1], Torben Ole Andersen[1], Morten Kjeld Ebbesen[2], Henrik Clemmensen Pedersen[1]

[1]Aalborg University
Pontoppidanstraede 111
9220 Aalborg East, Denmark
E-mail: vhd@et.aau.dk
Phone: +45 7159 7943

[2]Adger University
Jon Lilletuns vei 9
4879 Grimstad, Norway

ABSTRACT

This paper aims to evaluate the benefits and disadvantages of applying a digital hydraulic concept to actuate a knuckle boom crane. The standard cylinders of the knuckle boom crane will be substituted with multi-chamber cylinders of comparable size. The performance of one of the multi-chamber cylinders will be compared with the standard differential cylinder. The standard cylinder will be actuated with a constant pressure supply, a proportional directional valve and a proportional controller. Control performance and energy consumption for the two configurations have been considered. It is concluded that more research is needed into the control strategies in order to improve robustness and performance.

KEYWORDS: Digital hydraulics, Multi-chamber cylinder, Knuckle Boom cranes

## 1 Introduction

Hydraulic systems are a popular actuation solution in a number of industries. The high torque-to-size ratio is often stated as the reason for their popularity. Solution based on electric motors have to rely on often large gear ratios in order to achieve high torque/force low speed outputs. For this reasons applications intended to move large masses (lifting mechanisms, digging machines) or to work hard materials (steel rolling, some drilling applications) are attractive areas for hydraulics. Unfortunately the overall efficiency of the hydraulics transmission can be low depending on the work area. Specifically, part loading situations can be problematic due to the dissipative nature of throttling, which occurs over the proportional valve. This paper will examine the performance of digital hydraulic technology, specifically secondary controlled multi-chamber cylinders, on a large scale lifting mechanism-a knuckle boom crane.

Multi-chamber cylinder can experience problems with achieving smooth motion at low velocities, due to a smaller resolution of force outputs at low velocities [1]. This problem does depend on the mass of the system, what one decides to consider as low velocity and how often the pressures in the cylinder can be switched. The current state of the art in the control of multi-chamber cylinders involves the selection of an appropriate

pressure for each chamber and then throttling the flow with digital flow control units as in [1] or [2]. These controllers have achieved much smoother motion than the simpler controller, but they are generally more complex as well. The aim of this paper is to evaluate the performance of a simpler controller in order to establish the magnitude of possible problems for a system of this scale. This will be used to consider the need for more complex controllers and furthermore used as a baseline for the possibility of applying other digital hydraulic concepts. An often cited paper about secondary control of multi-chamber cylinders is [3]. In this paper the four chambers of a cylinder are pressurised to one of two pressure levels to produce different forces. The algorithm is shown to be very efficient, but some problems in the smoothness of the motion of the cylinder are evident. A different approach was applied by [4], were a 3 chamber cylinder is connected to 3 pressure lines. The middle pressure was used when switching from low to high pressure and vice-versa. This was shown to reduce the switching losses indtroduced by the compressibility of the hydraulic fluid. The focus of [4] was on energy efficiency, while the cylinder was part of a power take-off system in the Wavestar wave energy extraction concept. Due to this, trajectory tracking was not the main aim. In [5], Dengler et al propose to use multiple pressure lines in the control of a linear actuator in a wheel loader. The pump only maintains the pressure in the high pressure line. The control structure is based on a model prediction algorithm, which attempts to optimise the energy consumption of the pump over a horizon. In the cost function extracting energy from the high pressure line without charging the medium pressure line accumulator has a prohibitive cost. The algorithm in this paper will take inspiration from the one in [3], but an additional pressure line will be added as in [4]. Then the choice of middle pressure and controller parameters will be investigated. Furthermore the algorithm will be augmented with weights on the high pressure lines for the two larger chambers, in order to investigate the energy efficiency and position tracking of the controller if the middle pressure line is preferred in order to evaluate the possibility of applying an algorithm similar to [5]. In section 2, the dimensions of the knuckle boom crane are presented. In section 3 the model of the system is described. The control is discussed in section 4. The performance of the controllers will be presented and discussed in section 5. The paper ends with conclusions and future work in section 6.

## 2 Test Case

A two link knuckle boom crane has been selected as an investigation case. Knuckle boom cranes are popular in shipping and off-shore drilling industries. Knuckle boom cranes are characterised by high force, low speed operation modes. The large mass of the machine can result in a good match for digital hydraulics as it will naturally dampen some of the motion introduced by pressure pulsation. A picture of an example knuckle boom crane can be seen in Fig.1. The two cylinders connecting the column to the first link (inner jib) will be the focus of this paper. In the paper the two cylinder will considered as one cylinder of equivalent size and power, furthermore there are crane models of this size, which have a single cylinder actuating the inner jib e.g. the knuckle boom crane in [6]. The standard differential cylinder will be substituted with the three chamber multi-chamber cylinder seen in Fig.2. Each of the on-off valves in the circuit are assumed to have the same discharge coefficient and eigen frequency as the original proportional valve. The dimensions of the test case crane have been selected to reflect the scale of real knuckle boom crane. The dimensions used can be seen in table 1.

Figure 1: Knuckle Boom Crane example provided by National Oilwell Varco.©

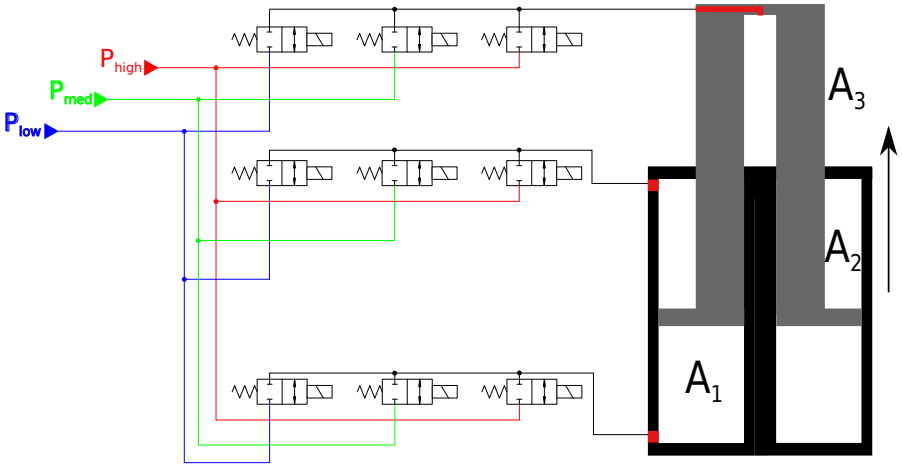


Figure 2: Representation of the multi-chamber cylinder used in the paper

| Body | Length [m] | Mass [kg] |
|---|---|---|
| Inner Jib | 10.8000 | 5600 |
| Outer Jib | 9.6000 | 2710 |
| Cylinder 1 | 1.755 | 1500 |
| Cylinder 2 | 1.33 | 750 |

Table 1: Crane dimensions

In this case a simple trajectory will be used where only the first cylinder will lift and lower the entire structure. Test trajectory for this situation can be seen in figure 3.

## 3 Model

The modelling section has been divided into a mechanical part and a hydraulic part. The mechanical part remains unchanged with both cylinder types.

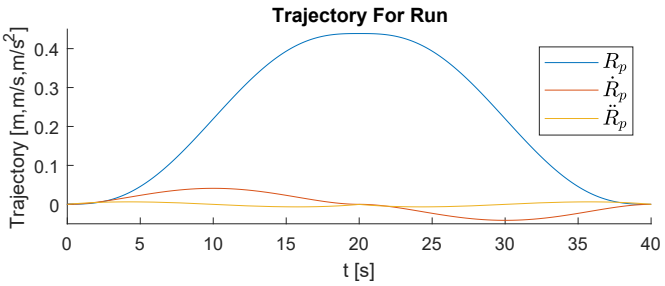


Figure 3: Reference Trajectory

### 3.1 Mechanical part

The non-linear equations describing the mechanical part of the model will be presented here in a very short form. According to [7] Newton's second law of motion for a multi body system can be expressed as:

$$\begin{bmatrix} M & D^T \\ D & 0 \end{bmatrix} \begin{bmatrix} \dot{v} \\ \lambda \end{bmatrix} = \begin{bmatrix} g_{ext} - b \\ \gamma \end{bmatrix} \tag{1}$$

where

| | |
|---|---|
| $M$ | is the matrix of masses and inertias around the center of mass of each link |
| $D$ | the constraint Jacobian found from the kinematic constraints of the system |
| $\lambda$ | is the vector of Lagrange multipliers |
| $\dot{v}$ | is a vector of the linear and rotational acceleration of the bodies |
| $g_{ext}$ | the vector of external forces, including gravity, Coriolis and cylinder forces |
| $b$ | contains the velocity cross product terms |
| $\gamma$ | is calculated from the derivation of the kinematic constraints of the system |

There are 7 bodies with 6 coordinates which means that $\dot{v} \in \mathbb{R}^{42}$ as seen in Eq. (2). In this case the bodies include the column(1), inner jib(2), the first cylinder (broken into two bodies 3 and 4), the outer jib (5), and the second cylinder (6, 7). This also makes the mass matrix $M \in \mathbb{R}^{42\times 42}$.

$$\dot{v} = \begin{bmatrix} \ddot{r}_1 \\ \dot{\omega}_1 \\ \vdots \\ \ddot{r}_7 \\ \dot{\omega}_7 \end{bmatrix} \quad q = \begin{bmatrix} r_1 \\ \Theta_1 \\ \vdots \\ r_7 \\ \Theta_7 \end{bmatrix} \tag{2}$$

The mechanical system is modelled as 7 revolute joints and two parallel constraints (forcing the cylinder and piston bodies to be parallel) similar to how a knuckle boom crane was modeled in [6]. This makes $D$ a $39 \times 42$ matrix. According to the Nikravesh method [7] the kinematic constraints of the system can be expressed as a non-linear function of the general coordinates of the multi body system. The theory states that when the constraints are not violated the kinematic constraints function $\Phi(q)$ returns zero. The specific equations for each joints are standard and can be found in [7]. The function can be differ-

entiated according to time to produce:

$$\Phi(q) = 0 \tag{3}$$
$$\dot{\Phi}(q,v) = Dv = 0 \tag{4}$$
$$\ddot{\Phi}(q,v,\dot{v}) = D\dot{v} + \dot{D}v = 0 \tag{5}$$
$$\gamma = D\dot{v} \tag{6}$$
$$\gamma = -\dot{D}v \tag{7}$$

This makes $\gamma$ a $39 \times 1$ vector. With these extra equation the number of unknowns and equations in Eq. (1) become equal and can be solved simultaneously. Finally $b$ is the cross product of velocities as seen in Eq. (8) and $b \in \mathbb{R}^{42}$.

$$b = \begin{bmatrix} 0^{3\times 1} \\ \tilde{\omega}_1 J_1 \omega_1 \\ \vdots \\ 0^{3\times 1} \\ \tilde{\omega}_7 J_7 \omega_7 \end{bmatrix} \tag{8}$$

where $\tilde{\omega}_1$ is the skew symmetric matrix constructed from the elements of $\omega_1$ in order to represent cross product. This concludes the modelling of the mechanical part.

### 3.2 Hydraulic part

The non-linear equations describing the change in pressure are

$$\dot{p} = C(Q_{move} + Q_{valve}) \tag{9}$$

where $\dot{p}$ is a vector of pressure gradients for each chamber. $C$ is the matrix of hydraulic capacitances. $Q_{move}$ is the change in chamber volumes due to the velocity of that piston as seen in Eq. (10). $Q_{valve}$ is the flow delivered by the valves. For the two cylinders with two chambers each, there are 4 pressure equations so $\dot{p} \in \mathbb{R}^4$. The bulk modulus of each chamber varies with the current pressure in the chamber. In Eq. (9), the vectors $Q_{move}$ and $Q_{valve}$ are defined as:

$$Q_{move} = \begin{bmatrix} -A_{1,1}\dot{x}_{p1} \\ A_{1,2}\dot{x}_{p1} \\ -A_{2,1}\dot{x}_{p2} \\ A_{2,2}\dot{x}_{p2} \end{bmatrix} \tag{10}$$

$$Q_{valve} = \begin{bmatrix} Q_{v,1}(u) \\ Q_{v,2}(u) \end{bmatrix} \tag{11}$$

$$Q_{v,1}(u) = \begin{cases} k_q u S(p_s - p_{1,1})\sqrt{(|p_s - p_{1,1}|} \\ k_q u S(p_{1,2} - p_t)\sqrt{(|p_{1,2} - p_t|} \end{cases} \quad u \geq 0$$
$$\begin{cases} k_q u S(p_s - p_{1,2})\sqrt{(|p_s - p_{1,2}|} \\ k_q u S(p_{1,1} - p_t)\sqrt{(|p_{1,1} - p_t|} \end{cases} \quad u < 0 \tag{12}$$

Here $A_{i,j}$ again stands for the area of the i-th cylinders j-th chamber. $\dot{x}_{p1}$ is the velocity of the 1st cylinder piston in the direction of the cylinder. $Q_{v,1}(u)$ is short for $Q_{v,1}(u,p,p_s,p_t)$,

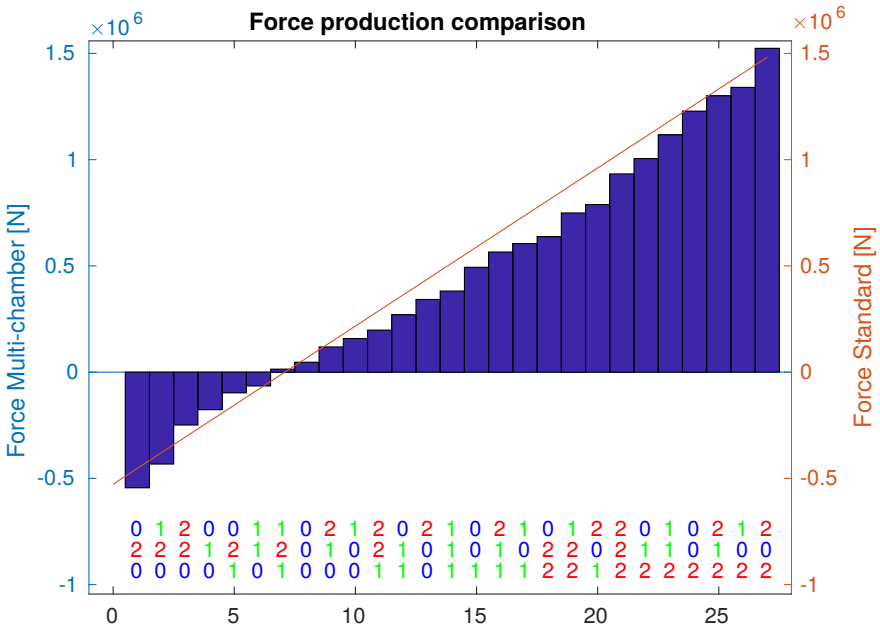


Figure 4: Forces the standard and multi-chamber cylinders can produce with the chosen pressures

which is the non-linear orifice equation describing the flow the valve delivers at the current spool position and pressure drops. In the case, where multi-chamber cylinders substitute the normal cylinders, some changes in the equations arise. The multi-chamber cylinder is chosen to have 3 chambers. Two chambers are delivering positive force (chosen as pushing) and one chamber delivers negative force (pulling). Three on-off valves are connected to each chamber of the cylinder. They connect the chamber to 3 constant pressure rails. A representation of the cylinder can be seen in Fig.2. The 3 chamber areas have been chosen in a ratio of $A_1 : A_2 : A_3 = 4 : 2 : 1$. The actual areas chosen so the cylinder produces a maximum positive force corresponding to the original cylinder. The three pressures are selected as $p_{high} = 22\ MPa$ , $p_{mid} = 9\ MPa$ and $p_{low} = 1\ MPa$. The middle pressure is selected through a parameter sweep discussed in section 4.2. The high and low pressure are close to the ones used in the normal cylinder case, so the two cylinder can be compared in force production easily. The comparison can be seen in Fig.4. Since there are three chambers the pressure gradient vector (9) becomes $\dot{p} \in \mathbb{R}^6$. The matrix of hydraulic capacitance also grows to a $6 \times 6$. The spools of the on-off valves can only take values as $u \in [0, 1]$. The discharge coefficient and eigen frequency of the on-off valves are considered to be the same as the proportional ones.

## 4 Control

### 4.1 Classic control

A standard Proportional controller is used on the standard cylinders. The non-linear model has been linearised around cylinder middle position, which should be close to the lowest eigen-frequency of the cylinder. A velocity feedforward term is added to improve the trajectory tracking capabilities of the controller. A gain scheduling is introduced with a

gain and a velocity feedforward term for each direction of movement.

### 4.2 Secondary Controlled Multi-chamber cylinder

For the secondary controlled multi-chamber cylinder situation a simple force controller is chosen. The controller was originally suggested in [3] and since then has been augmented and improved with digital flow control units as in [1]. In [3], the controller switches between two constant pressure rails and the cylinder has four chambers. In [8] it was shown that having a third pressure rail with a value between the maximum and minimum pressure can result in a more efficient performance. The reason is that switching between pressures was identified as the largest source of losses for multi-chamber cylinders. The switching losses for a chamber which switches from one pressure $p(t)$ to another pressure $p_s$ have been defined by [8] as:

$$E_{loss,\beta} = E_{supply} - E_{vol} = \int_0^\infty p_s Q(t)dt - \int_0^\infty p(t)Q(t)dt \tag{13}$$

These losses occur, because the flow exiting a constant pressure rail is the same as the one entering the cylinder chamber. Since fluid power is defined as the flow times the pressure at which it is delivered, the power exciting the pressure rail is larger than the one entering the cylinder. The excess energy is converted to heat over the valve. With further mathematical manipulation Hansen et al [8], prove that the losses for the chamber depend on the initial pressure $p_0$ and the end pressure $p_1$, the chamber volume $V$ and the bulk modulus $\beta$:

$$E_{loss,\beta} = \frac{1}{2}(p_1 - p_0)^2 \frac{V}{\beta} \tag{14}$$

If the difference between $p_1$ and $p_0$ is small the switching loss is also small. Furthermore, because the pressure difference appears in the power of two in Eq. (14), switching to an intermediate pressure before switching to a high pressure can reduce losses considerably. The control algorithm can be expressed as choosing a control combination $u_i$ where $i$ is one of the 27 possible combinations, which minimises a cost function seen Eq. (15) . Each $u_i$ is a vector of 9 binary values for the 9 valves - $u_i = [u_{i,1}, u_{i,2}, \cdots, u_{i,9}]$.

$$u_i = \underset{u_i}{argmin} \{|F_{ref} - F_i| + W u_{change}\} \quad i = 1, \cdots, 27 \tag{15}$$

where

| | |
|---|---|
| $F_{ref}$ | is a force reference |
| $F_i$ | is the force produce by valve combination $i$ |
| $W$ | is a weight to be chosen |
| $u_{change}$ | is a binary values, which is equal to 1 if combination $i$ is different from the current valve combination |

The control algorithm selects one of the $3^3 = 27$ valve combinations (3 chambers and 3 possible pressures), which would produce a different force $F_i$. The aim is for this force to be as close as possible to a force reference. The force reference is obtained by using the non-linear model and the reference trajectory to determine a feedforward signal as seen in Eq. (17). In order to account for the fact that the discontinuous controller will not be

able to follow the continuous force trajectory perfectly, a position and a velocity error are added to the reference as seen in Eq. (18)

$$e = x_{ref} - x_p \quad \dot{e} = \dot{x}_{ref} - \dot{x}_p \tag{16}$$

$$F_{ff} = D(x_{ref})\ddot{x}_{ref} + C\dot{x}_{ref} + G(x_{ref}) \tag{17}$$

$$F_{ref} = F_{ff} + G_1 e + G_2 \dot{e} \tag{18}$$

where $e$ and $\dot{e}$ are position and velocity errors, respectively. $F_{ff}$ is a feedforward term calculated from the non-linear 1 degree model of the system in actuator space. $D(x)$ and $G(x)$ are functions for mass and gravitational force as seen by the cylinder. $C$ is the viscous friction coefficient of the cylinder. $G_1$ and $G_2$ are gains. As mentioned before pressurising and de-pressurising chambers is associated with losses. That is the purpose of the "W" term. To select the middle pressure level and the weight on switching a parameter sweep is performed. The energy used to follow the trajectory as a function of weight and middle pressure can be seen in Fig.5. The root-mean-square of the position error can be seen in Fig.6. Here the energy used to track the trajectory is defined as

$$E_{sum} = \int_0^{t_{end}} p_{high} Q_{high}(t)dt + \int_0^{t_{end}} p_{med} Q_{med}(t)dt + \int_0^{t_{end}} p_{low} Q_{low}(t)dt \tag{19}$$

where $Q_s$, $Q_{med}$ and $Q_{low}$ are the flows exiting the pressure lines. It can be seen that

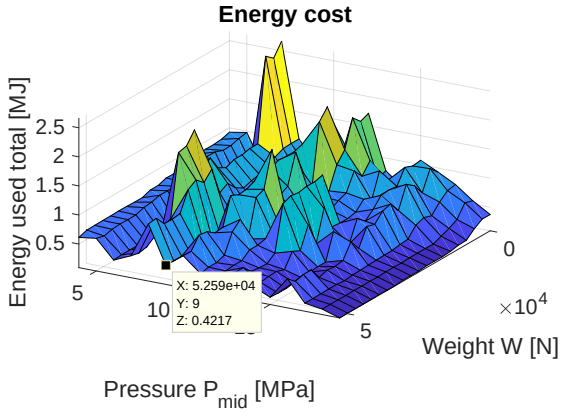


Figure 5: Energy used total as a function of weight and mid pressure

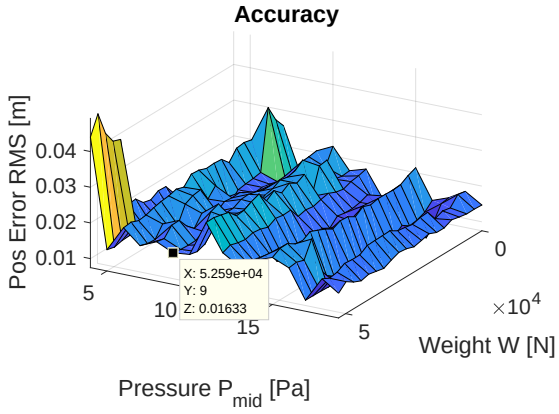


Figure 6: Tracking accuracy as a function of weight and mid pressure

there are multiple points with similar costs. Furthermore it can be seen that certain combinations of middle pressure and switching weight result in very poor performance. For most cases the middle pressure has a much larger effect on the efficiency of the system, compared with the effect of a different weight on the switching. The highlighted point is selected with a middle pressure $p_{mid} = 9\ MPa$ and a weight $W = 52590\ N$.
Since the valve are not infinitely fast first a "close valves" command is given and after 25 *ms* the "open valves" command is given. After another 25 *ms* a new combination is chosen. According to this the controller chooses a new combination every 50 *ms* and so it can be considered to be running at 20 $Hz$.

### 4.3 Augmented controller

A lot of attention within digital hydraulics has been devoted to minimising losses. Considering Eq. (13), changing the pressure level of a chamber is not desired. But in [5],

there is a preference for using the middle chamber pressure, because that pressure line is connected to an accumulator which stores regenerated energy. In order to examine how the algorithm performs if the middle pressure line is preferred an additional weight has been added to the controller. The augmented algorithm is:

$$u_i = \underset{u_i}{argmin} \left\{ |F_{ref} - F_i| + W u_{change} + W_{large} u_{i,3} + W_{large} u_{i,6} \right\} \quad i = 1, \cdots, 27 \tag{20}$$

where $u_{i,3}$ and $u_{i,6}$ are the valves used to connect the high pressure rail to chambers A and B. $W_{large}$ is an arbitrary weight chosen large enough to prevent the controller from using combination with higher pressures. Once again a parameter sweep has been conducted to determine how the middle pressure and the weight on switching will affect the performance. The effect on the energy used to follow the trajectory can be seen in Fig.7. The root-mean-square of the position error can be seen in Fig.8. It can be seen that the

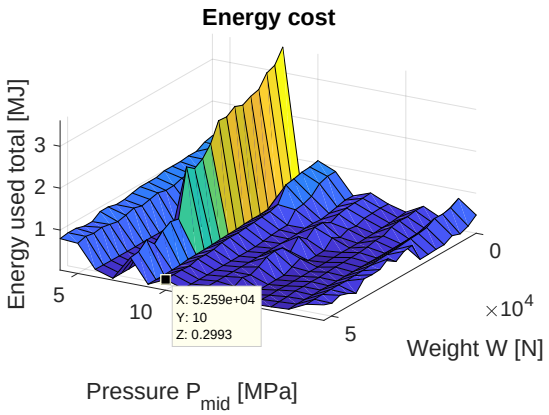


Figure 7: Energy used total as a function of weight and mid pressure

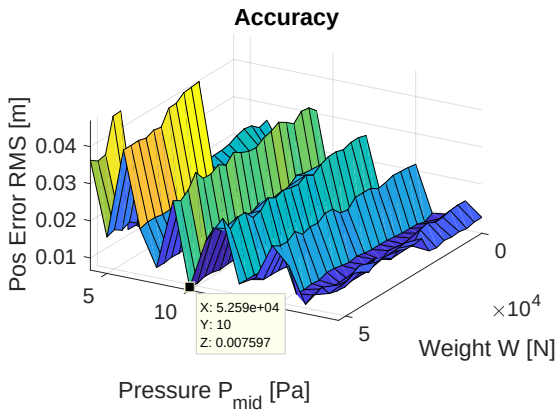


Figure 8: Tracking accuracy as a function of weight and mid pressure

pressure level has an even larger effect on the costs. Furthermore better performance can generally be obtained by using a larger medium pressure. A point close to the one used for the original controller is chosen. The medium pressure is raised from 9 *MPa* to 10 *MPa*, because of the large tracking error at 9 *MPa*. The large tracking error for some pressures is introduced, because the controller prefers not to use the high pressure line in chambers A and B. This reduces the force resolution. In the cases where the error is not increased, the available forces match the trajectory better.

## 5 Results

The trajectory tracking of the 3 controllers can be seen in Fig.9. Better tracking performance can be achieved by either selected a different pressure or increasing the gains $G_1$ and $G_2$. A different pressure was not selected, because the point chosen was apparently optimal according to Fig.5 and Fig.6. It is obvious that the proportional controller follows the trajectory better.

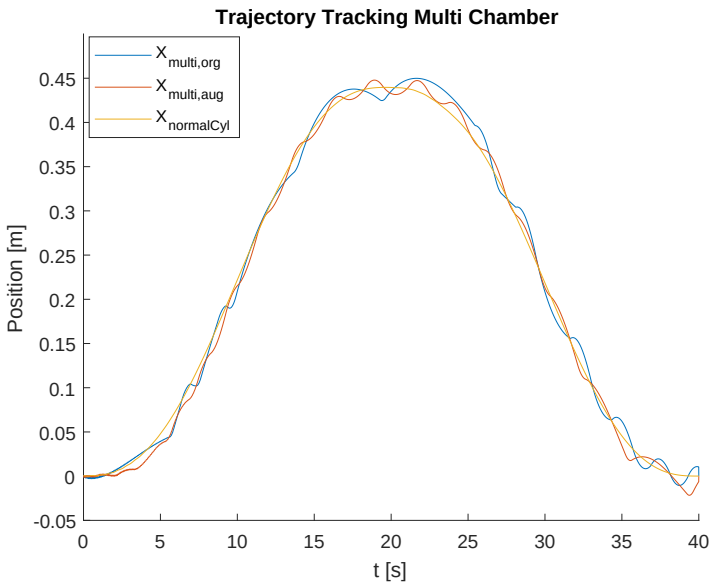


Figure 9: Trajectory tracking with the different controllers

The energy used to follow the trajectory by the 3 controllers can be seen in Fig.10. Both multi-chamber cylinders use less energy than the standard cylinder. But they use nearly the same amount of energy as each other.

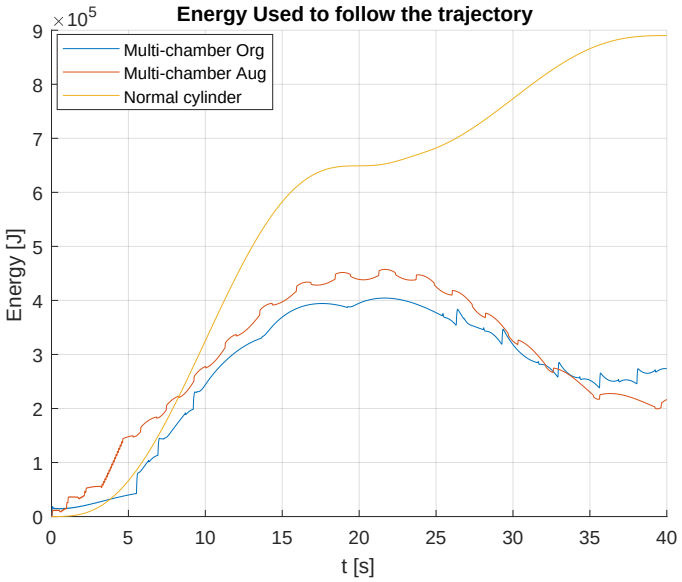


Figure 10: Energy used to follow the trajectory

To investigate the difference between the controllers the energy used by each chamber can be seen in Fig.11 for the original controller and in Fig.12 for the augmented one. It can be seen that the original controller uses more energy through chamber A but also returns more energy through chamber B. This is because both A and B chamber are connected to the same high pressure. In comparison chamber A in the augmented controller uses nearly half the energy, but very little energy is returned through chamber B. During the lowering motion, chamber A in original controller is switched between high and medium pressure. This reduces the efficiency of energy regeneration.

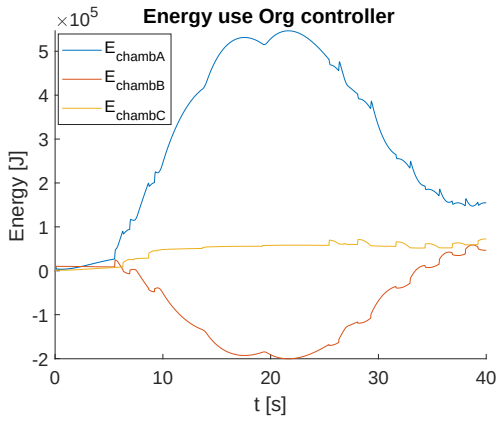


Figure 11: Energy used to follow the trajectory by chamber

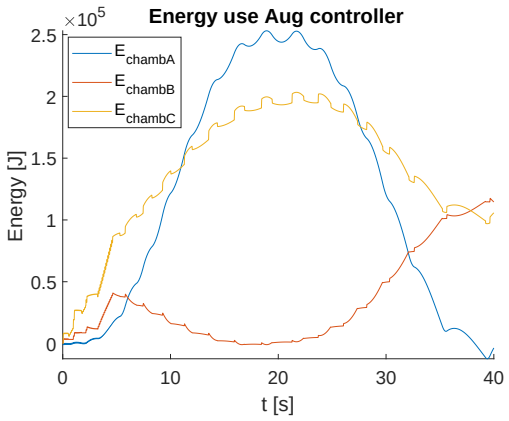


Figure 12: Energy used to follow the trajectory by chamber

The chamber pressures can be seen seen in Fig.13 and Fig.14. Fig.13 shows that for a large part of the trajectory the pressures do not change for the original controller. Furthermore both of the large chambers are connected to the high pressure. The lack of switching of the large chamber with few switches of the smallest chamber to middle pressure explain why this the middle pressure and weigth were determined as near optimal. In comparison the augmented controller switches more often, but it is the second and third chambers that are switching. This enables chamber A to regenerate all of the energy it had used in the first half of the trajectory. Very little energy is regenerated through Chamber B for the first half of the trajectory and it uses a lot of energy in the second half. Most of the energy is lost due to the switching in chambers B and C. The large amount of switching just before the 5 second mark is due to the velocity feedback. Reducing or removing it completely avoided this problem, but the overall tracking of the controller was much poorer.

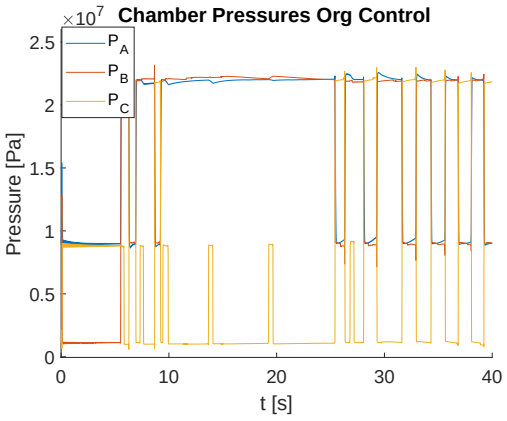


Figure 13: Pressures used to follow the trajectory

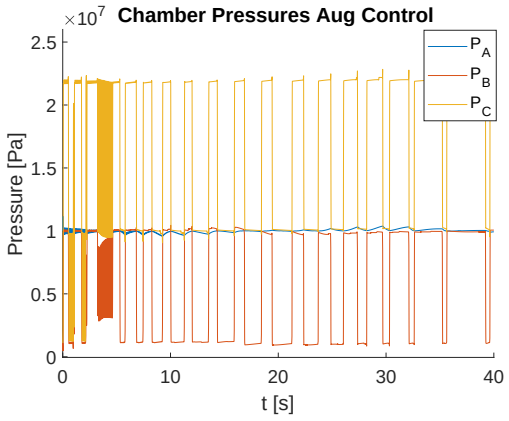


Figure 14: Pressures used to follow the trajectory

The forces used by the multi-chamber cylinder force controllers can be seen in Fig.15. It can be seen that the force produced by the multi-chamber cylinder with the original controller is very close to the predetermined feedforward signal. It can be seen that when lowering the jib, the original controller produces huge force spikes. This is due to dangerous switching combinations that involve switching the pressure of all the chambers simultaneously. In this paper, it has been assumed that the valves have no uncertainty in

closing time. In reality this is not the case and it has been shown that the problem can be much larger and it is difficult to avoid [9]. To test the robustness of the controllers they

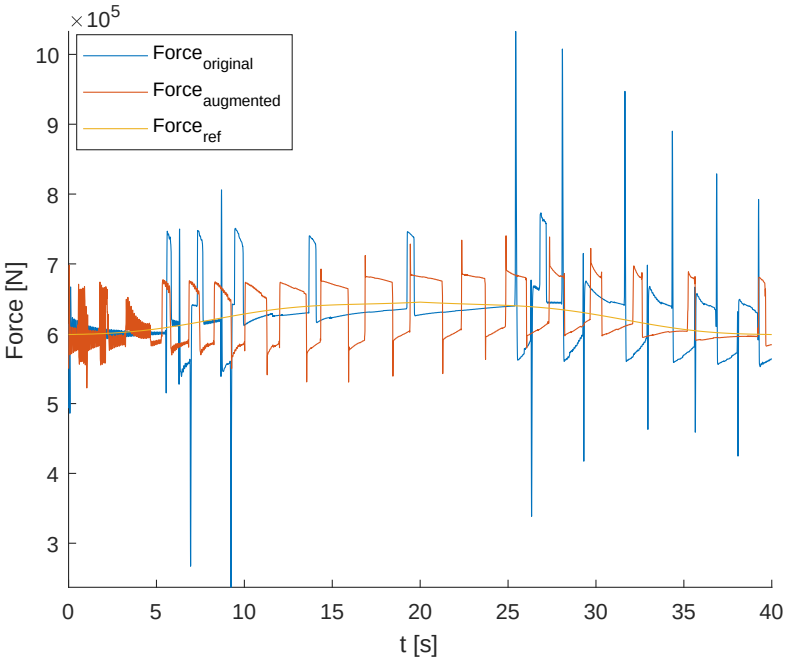


Figure 15: Forces applied by the different controllers

have been tested under different conditions. The conditions involve a trajectory which is two times faster, and a trajectory that is two times slower. Then the weight and inertia of the outer jib have been doubled and the three trajectories are run again with both controllers. The results can be seen in table 2 and table 3.

Results with original load

| | Energy used [MJ] | | | Error RMS [m] | | |
|---|---|---|---|---|---|---|
| Velocity | Normal | Increased | Decreased | Normal | Increased | Decreased |
| Normal Cyl | 0.89007 | 0.89308 | 0.88867 | 0.002 | 0.0026 | 0.0013 |
| Contr Org | 0.27357 | 0.28364 | 0.71907 | 0.0097 | 0.0113 | 0.0098 |
| Contr Aug | 0.21672 | 0.14764 | 0.22810 | 0.0074 | 0.0124 | 0.0074 |

Table 2: Result of simulations with different trajectories

## 6 Conclusion and future work

Some conclusions can be made based on the results in this paper.

- Energy wise the knuckle-boom crane is a good fit for digital hydraulic technology.
- The tracking performance of the multi-chamber cylinder force controllers is not satisfactory, because for instance due to the lengths of the links an error of 0.0188 $m$ as seen in Fig.9, result in a deviation of $\approx 0.45$ $m$ of the tool center point of the crane.

Results with increased load

| | Energy used [MJ] | | | Error RMS [m] | | |
|---|---|---|---|---|---|---|
| Velocity | Normal | Increased | Decreased | Normal | Increased | Decreased |
| Normal Cyl | 0.89455 | 0.91036 | 0.89207 | 0.0054 | 0.0087 | 0.0028 |
| Controller Org | 0.47680 | 0.39424 | 0.79168 | 0.0078 | 0.0090 | 0.0088 |
| Controller Aug | 0.37959 | 0.28645 | 0.65295 | 0.0118 | 0.0180 | 0.0133 |

Table 3: Result of simulations with different trajectories and increased load

- Tracking wise the two multi-chamber controllers are robust in the sense that changing the load and velocity of the trajectory does not degrade the tracking performance considerably.
- The energy use of the multi-chamber force controllers cannot be said to be robust as seen in table 2, specifically the result with a decreased velocity trajectory and the original controller.
- The choice of middle pressure level and switching weight is not trivial, because their effect on the energy and error cost are non-linear as seen in the parameter sweep plots Fig.5, Fig.6,Fig.7 and Fig.8.
- If the middle pressure line changes significantly during the operation of the system the performance of the controller may also change, as seen in the results of the parameter sweeps in Fig.6 and Fig.8.
- The weight on switching is meant to prevent chattering situations such as the one in Fig.14, but this cannot be guaranteed with a preselected constant weight.
- Slower trajectories with a larger load may result in more switching which can bring the overall efficiency of the controller down considerably as seen in table 3.
- The size of the chambers needs to be taken into account when switching as shown in [8] and [10].

Based on these consideration a model predictive controller, which can optimise over a certain horizon, might be a good solution. In [11] a model predictive controller is used to drive a multi-chamber cylinder and the results are compared with a controller similar to [4] and the ones used in this paper. The model predictive controller showed better tracking performance while still using less energy.
Also in [6] a knuckle-boom crane with flexible bodies is considered. It should be investigated if any resonance modes might be excited in the structure.
Further it should be investigated if it is beneficial to have more pressure rails. The increased force resolution should result in less switching. It appears that a tendency has emerges towards towards multiple pressures, but normal cylinder. Instead of 3 pressure lines Huova et al. propose 100 in [10], but probalby due to practical reasons a prototype with 7 pressure line is tested instead and 6 are used in [12]. Since the pressure difference between the steps is smaller the compressibility losses are reduced. This is due to some extent because the smaller force steps result in smaller losses, when switching between them, but also as seen Fig.15 if a force combination is very close to the force reference the controller doesn't need to switch as often. Adding an additional pressure line has a much

smaller effect on the force resolution, than an additional chamber. On the other hand having more than two chambers in a cylinder introduces force steps, which can result in a large force uncertainty while switching.

## 7 ACKNOWLEDGMENT

The research in this paper has received funding from The Research Council of Norway, SFI Offshore mechatronics, project number 237896/O30.

## References

[1] M. Huova, A. Laamanen, and M. Linjama, "Energy efficiency of three-chamber cylinder with digital valve system," *International Journal of Fluid Power*, vol. 11, no. 3, pp. 15–22, 2010.

[2] K. Pettersson, K. Heybroek, P. Mattsson, and P. Krus, "A novel hydromechanical hybrid motion system for construction machines," *International Journal of Fluid Power*, vol. 18, no. 1, pp. 17–28, 2017.

[3] M. Linjama, H. Vihtanen, A. Sipola, and M. Vilenius, "Secondary controlled multi-chamber hydraulic cylinder," in *The 11th Scandinavian International Conference on Fluid Power, SICFP*, vol. 9, 2009, pp. 2–4.

[4] R. H. Hansen, M. M. Kramer, and E. Vidal, "Discrete displacement hydraulic power take-off system for the wavestar wave energy converter," *Energies*, vol. 6, no. 8, pp. 4001–4044, 2013.

[5] P. Dengler, M. Geimer, and R. v. Dombrowski, "Deterministic control strategy for a hybrid hydraulic system with intermediate pressure line," in *ASME/BATH 2012 Symposium on Fluid Power and Motion Control*. American Society of Mechanical Engineers, 2012, pp. 334–347.

[6] M. K. Bak and M. R. Hansen, "Analysis of offshore knuckle boom crane-part one: modeling and parameter identification," *Modeling, Identification and Control*, vol. 34, no. 4, p. 157, 2013.

[7] P. E. Nikravesh, *Computer-aided analysis of mechanical systems*. Prentice-Hall, Inc., 1988.

[8] R. H. Hansen, T. O. Andersen, and H. C. Perdersen, "Analysis of discrete pressure level systems for wave energy converters," in *Fluid Power and Mechatronics (FPM), 2011 International Conference on*. IEEE, 2011, pp. 552–558.

[9] A. Laamanen, M. Linjama, and M. Vilenius, *On the pressure peak minimization in digital hydraulics*. Tampere University of Technology, 2007, pp. 107–121, contribution: organisation=iha,FACT1=1.

[10] M. Huova, A. Aalto, M. Linjama, K. Huhtala, T. Lantela, and M. Pietola, "Digital hydraulic multi-pressure actuator–the concept, simulation study and first experimental results," *International Journal of Fluid Power*, pp. 1–12, 2017.

[11] A. Hansen, M. Asmussen, and M. Bech, "Energy optimal tracking control with discrete fluid power systems using model predictive control," *submitted to The Ninth Workshop on Digital Fluid Power*, 2017.

[12] M. Huova, A. Aalto, M. Linjama, and K. Huhtala, "Study of energy losses in digital hydraulic multi-pressure actuator," in *The 15th Scandinavian International Conference on Fluid Power*, 2017.